PCCP

Accepted Manuscript

ROYAL SOCIETY OF CHEMISTRY

www.rsc.org/pccp

Journal Name

RSCPublishing

ARTICLE

Interfacial charge-transfer transitions in the TiO_2-benzenedithiol complex with Ti-S-C linkages

Jun-ichi Fujisawa,* Ryuki Muroga and Minoru Hanaya

Cite this: DOI: 10.1039/x0xx00000x

Received 00th January 2012,
Accepted 00th January 2012

DOI: 10.1039/x0xx00000x

www.rsc.org/

Interfacial charge-transfer (ICT) transitions between organic materials and inorganic semiconductors are a new mechanism for light absorption by organic-semiconductor interfaces. ICT transitions cause one-step interfacial charge separation without loss of energy. This feature is potentially useful to realize efficient organic-inorganic hybrid solar cells. ICT transitions have been examined employing titanium dioxide (TiO_2) nanoparticles chemisorbed with π-conjugated molecules via Ti-O-C linkages. Here, we report ICT transitions in the TiO_2 and 1,2-benzenedithiol (BDT) complex with Ti-S-C linkages. BDT adsorbs on TiO_2 by the bridging bidentate coordination of the sulfur atoms to surface titanium atoms. The TiO_2-BDT complex shows ICT transitions fromthe BDT moiety to the conduction band of TiO_2 in the visible region. The ICT transitions occur by orbital overplaps between the d orbitals of the surface titanium atoms and the π orbitals of the benzene ring. Our density-functional-theory (DFT) analysis reveals that the 3p valence orbitals of the sulfur bridging atoms contributes to more than 50% of the highest occupied molecular orbital (HOMO) and the 3d-3p(sulfur)-π interaction via the Ti-S-C linkage enhances the electronic mixing between the titanium atoms and benzene moiety as compared to the 3d-2p(oxygen)-π via the Ti-O-C linkage. This result indicates the important role of the heavier-atom linkers for strong organic-inorganic electronic couplings.

Introduction

Interfacial electronic transitions between organic materials and inorganic semiconductors are a novel mechanism for light absorption by organic-semiconductor interfaces. In contrast to electronic transitions in materials, interfacial electronic transitions can generate photocarriers at the interface selectively, as illustrated in Fig. 1. There are two kinds of interfacial electronic transitions with and without charge-transfer nature.[1] The interfacial charge-transfer (ICT) transitions perform direct photoinduced charge separation without loss of energy between organic materials and inorganic semiconductors. This direct charge separation is potentially useful to eliminate the energy loss in conventional charge separation processes in organic-inorganic hybrid solar cells for effcient photovoltaic conversions, as proposed in the literature.[2,3] So far, ICT transitions have been investigated in several hybrid materials formed from TiO_2 nanoparticles and π-conjugated molecules or polymers with Ti-O-C chemical linkages.[4-6] In these hybrid materials, ICT transitions occur by orbital interactions between TiO_2 and π-conjugated molecules via the Ti-O-C linkages. Therefore, the ICT transitions are governed by the linkage part.

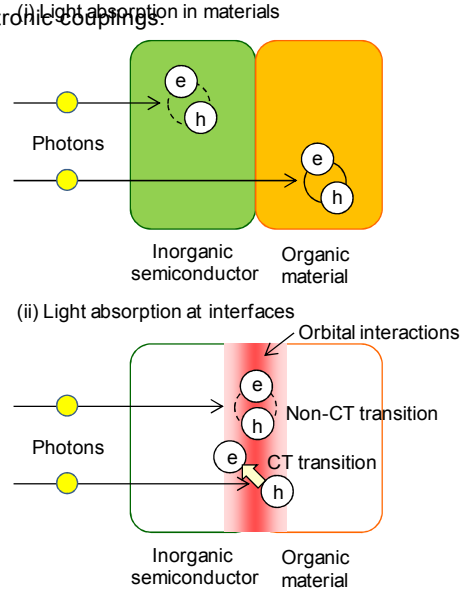

Fig. 1. Schematic pictures of two light absorption mechanisms. (a) light absorption in materials and (b) light absorption at interfaces between organic materials and inorganic semiconductors.

In this paper, we report ICT transitions in the TiO_2 and 1,2-benzenedithiol (BDT) complex with Ti-S-C linkages.[7]

Methods

Experimental

1,2-benzenedithiol (BDT) was purchased from Sigma-Aldrich and used without further purification. The TiO_2-BDT sample was prepared by immersing anatase TiO_2 nanoparticles (P90, Aerosil) in the 10 mM BDT solution (solvent: acetonitrile) for ca. 24 hours at room temperature. Then, the TiO_2-BDT sample was filtered and washed with acetonitrile and then vacuum-dried. The TiO_2 (blank) sample was prepared in the same manner without BDT. Absorption and diffuse reflectance spectra were measured by means of a UV-VIS-NIR spectrophotometer (V-670, JASCO). FT-IR spectra were measured by means of a FT-IR spectrometer (iS10, Nicolet) with a diamond ATR crystal.

Electrochemical photovoltaic cells were fabricated by the following method. Mesoporous TiO_2 electrodes (active area: 4×4 mm^2) were prepared by screen-printing of four kinds of TiO_2 nanoparticle pastes, HT/SP, T/SP, D/SP, and R/SP (Solaronix SA Co.) with different particle sizes on F-doped SnO_2 (FTO) transparent conducting glass substrates (Nippon Sheet Glass Co.) with sheet resistance of 10 Ω per square and sintering them at 773 K for 30 min. The sintered TiO_2 electrodes were treated by $TiCl_4$ for improvement of electric contacts between nanoparticles and rinsed with deionized water and ethanol, then sintered at 773 K for 30 min again. The thickness of the TiO_2 electrodes was set to ca. 18 μm. The TiO_2 electrodes were immersed in the 3.2 mM BDT solution (solvent: acetonitrile) at room temperature. Photovoltaic cells were fabricated using the TiO_2-BDT electrode, a Pt-sputtered FTO glass counter electrode, I^-/I_3^- redox couple electrolyte (ca. 2 M LiI, 0.025M I_2 /acetonitrile), and a polymer spacer film (thickness: 30 μm, Surlyn®film). Incident photon-to-current conversion efficiency (IPCE) excitation spectra were measured by means of a Hypermonolight system (SM-250E, Bunkoukeiki) with a calibrated silicon photodiode (S1337, Bunkoukeiki).

Computational

For theoretical analyses, we constructed a model complex based on an anatase TiO_2 nanocluster, $[Ti_{12}O_{20}(OH)_6(\mu\text{-}S)_2$-benzene] as a model complex of anatase TiO_2 nanoparticles chemisorbed with BDT, as will be described later. The TiO_2 cluster was built using the reported X-ray experimental result[8,9] of bulk anatase TiO_2. The optimized structure in vacuum was calculated with density functional theory (DFT)[10] employing the B3LYP functional[11] and 6-31G(d,p)[12] basis set. In the calculation, the coordinates of all the titanium and oxygen atoms were frozen to those of anatase TiO_2, maintaining the anatase structure. The vibrational and electronic excitation spectra of the optimized model complex in vacuum were calculated with DFT and time-dependent DFT (TD-DFT)[13],

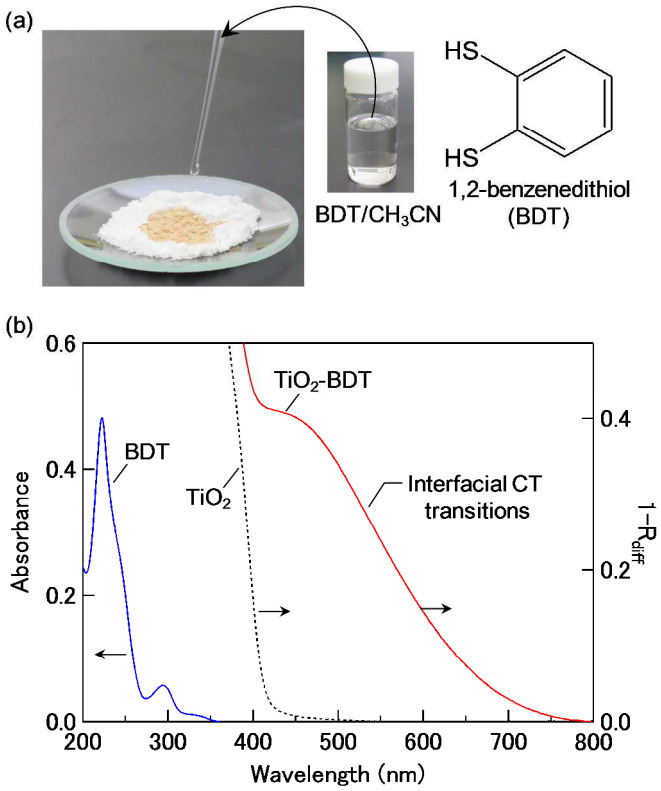

Fig. 2. (a) Coloration of anatase TiO_2 nanoparticles by addition of the colorless BDT solution and (b) diffuse reflectance spectra of TiO_2 nanoparticles before (black dashed curve) and after (red curve) immersion in the BDT solution (solvent: acetonitrile) together with the absorption spectrum (blue curve) of the BDT solution.

respectively, using the same functional and basis set. All the calculations were performed by using a Gaussian 09 software[14]. Total and partial densities of states were calculated by using a GaussSum software.[15]

Results and discussion

As shown in Fig. 2(a), we observed that TiO_2 nanoparticles become colored by the addition of the colorless BDT solution (solvent: acetonitrile) at room temperature. Fig. 2(b) shows the diffuse reflectance spectrum of TiO_2 nanoparticles immersed in the BDT solution. TiO_2 treated with BDT showed a broad absorption band in a longer wavelength region than the inter-band absorption ($\lambda \lesssim 400$ nm, $E_g = 3.2$ eV) of TiO_2 and intra-molecular absorption of BDT in the near UV region. The coloration and appearance of the broad absorption band suggest the complex formation between TiO_2 and BDT.

Fig. 3(a) shows FT-IR spectra of TiO_2, BDT and the TiO_2-BDT complex. The TiO_2-BDT complex showed several broad and sharp vibrational peaks, as shown in Fig. 3(c). Three broad peaks were observed around 1458, 1550, and 1633 cm^{-1}. Relatively sharp peaks were observed at 1263 (weak), 1437 (strong), and 1567 cm^{-1} (weak). TiO_2 nanoparticles (blank) exhibited three broad absorption bands at 1439, 1550, and 1637 cm^{-1}, as shown in Fig. 3(a). These bands are attributed to

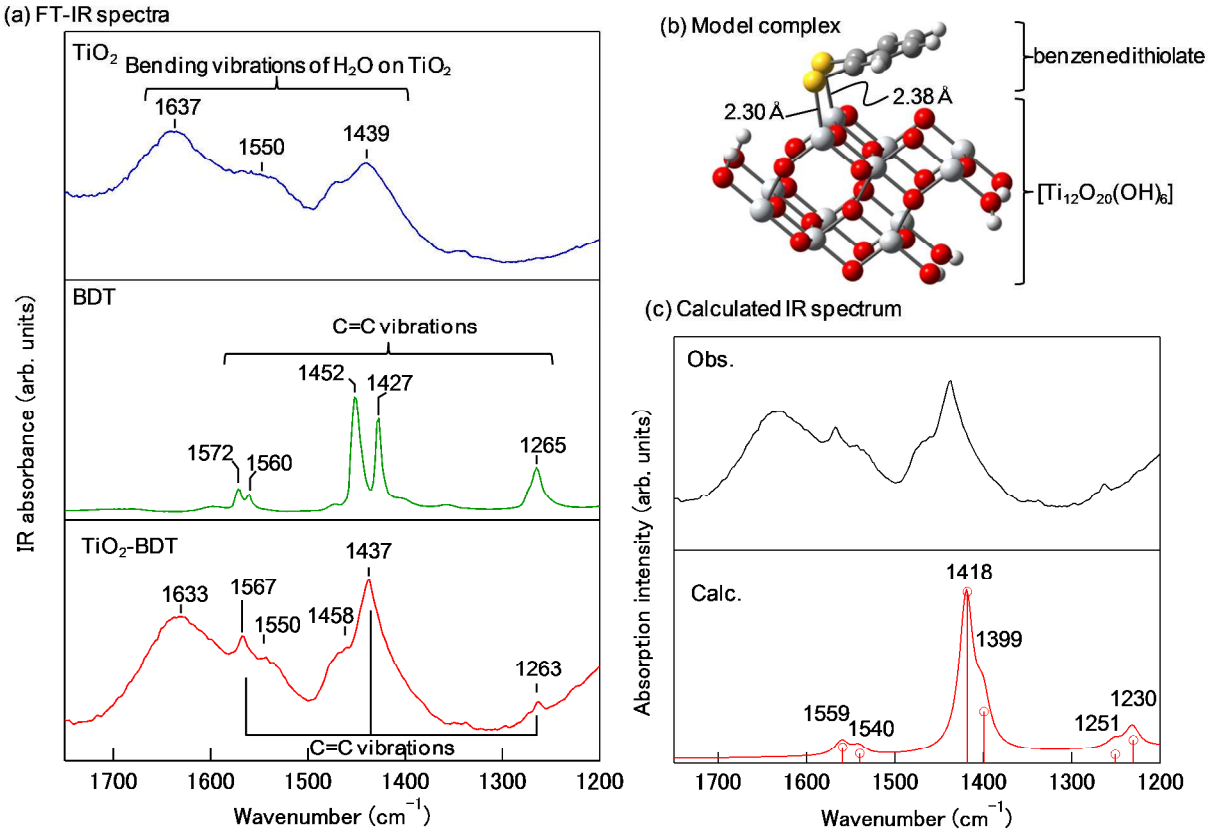

Fig. 3. (a) FT-IR spectra of TiO_2 (blue), BDT (green) and TiO_2-BDT (red) and (b) optimized structure and (c) calculated IR spectrum of $[Ti_{12}O_{20}(OH)_6(\mu\text{-}S)_2\text{-benzene}]$. The calculated wavenumbers were corrected using a scaling factor of 0.9613. The spectrum was obtained by convoluting the line spectrum with Gaussian absorption line-shapes with a full-width at a half maximum of 20 cm^{-1}. Gray: carbon, small white: hydrogen, red: oxygen, large white: titanium, and yellow: sulfur atom.

bending vibrations of water molecules physisorbed on TiO_2.[16] As the broad bands are similar to those of the TiO_2-BDT sample, the broad bands observed for TiO_2-BDT are assigned to water molecules physisorbed on TiO_2. On the other hand, BDT showed sharp C=C vibrational peaks at 1265 (weak), 1427 (strong), 1452 (strong), 1560 (weak), and 1572 cm^{-1} (weak), as shown in Fig. 3(b). As these peaks well correspond to the sharp peaks in the TiO_2-BDT complex, the three sharp peaks observed for TiO_2-BDT are assigned to the C=C vibrational peaks of adsorbed BDT molecules. By the adsorption of BDT on TiO_2, the double-peak structures in the highest and intermediate wavenumber regions for free BDT changed to a single peak structure and the relative intensity of the lowest wavenumber peak was considerably reduced.

In order to theoretically analyze the adsorption structure of BDT on TiO_2, we constructed a model complex based on an anatase TiO_2 nanocluster $[Ti_{12}O_{20}(OH)_6(\mu\text{-}S)_2\text{-benzene}]$, in which BDT adsorbs on TiO_2 via the bridging bidentate Ti-S-C coordination, as shown in Fig. 3(b). We examined the bridging bidentate Ti-S-C coordination as one of the possible adsorption structures.[17] The optimized structure was calculated by DFT with freezing the coordinates of all the titanium and oxygen atoms to those of anatase TiO_2 in order to maintain the anatase structure. As shown in Fig. 3(b), the Ti-S bond length was estimated to be 2.30 and 2.38 Å. The optimized Ti-S bond lengths are close to the reported values (2.35 – 2.46 Å)[20] of the Ti-BDT complexes.

Fig. 3(c) shows the calculated IR spectrum of the optimized $[Ti_{12}O_{20}(OH)_6(\mu\text{-}S)_2\text{-benzene}]$. The calculated vibrational wavenumbers were corrected using the reported scaling factor of 0.9613 for the B3LYP functional and 6-31G(d) basis set.[21] The model complex shows C=C vibrational peaks at 1230 (weak), 1251 (weak), 1399 (weak), 1418 (strong), 1540 (weak), and 1559 cm^{-1} (weak). The convoluted spectrum was obtained using Gaussian line-shapes with a full-width at a half maximum of 20 cm^{-1}. This spectrum is in good agreement with the observed one, well reproducing the above-mentioned changes of the C=C vibrational peaks by the adsorption onto TiO_2. This result suggests the validity of the bridging bidentate Ti-S-C coordination.

We calculated a hundred of electronic excitations in the optimized structure of the model complex by TD-DFT, as shown in Fig. 4(a). The calculated spectrum was obtained by convoluting the line spectrum with Gaussian line-shapes tentatively assuming a full-width at a half maximum of 5000 cm^{-1}. The convoluted spectrum is in accordance with the observed diffuse reflectance spectrum. The calculation result indicates that a number of electronic excitations occur in the

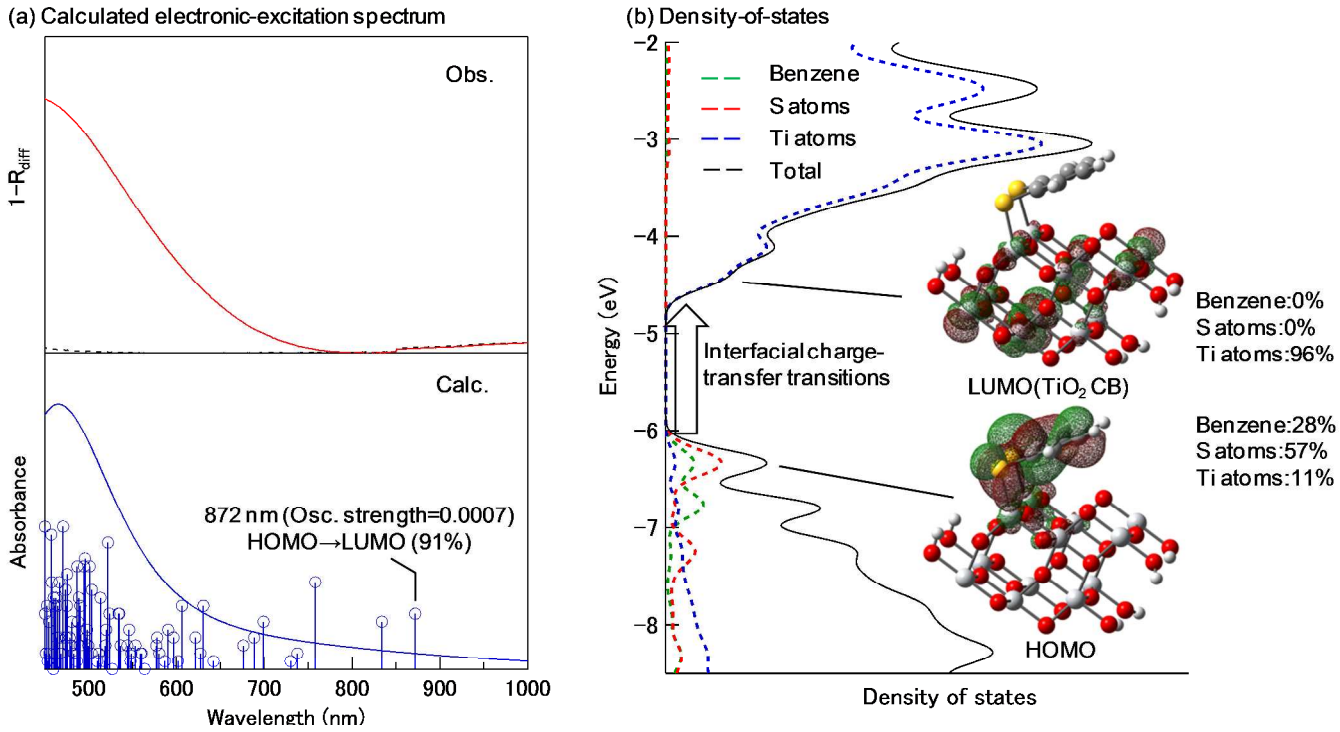

Fig. 4. (a) Experimental absorption spectrum (red) of the TiO_2-BDT complex and calculated electronic excitation spectrum (blue) of the model complex $[Ti_{12}O_{20}(OH)_6(\mu\text{-}S)_2$-benzene] and (b) total and partial densities of states of $[Ti_{12}O_{20}(OH)_6(\mu\text{-}S)_2$-benzene] together with electronic distributions (|isovalue| = 0.02) of the HOMO and LUMO. The calculated spectrum was obtained by convoluting the line spectrum with Gaussian absorption line-shapes with a full-width at a half maximum of 5000 cm^{-1}. The total and partial densities of states were obtained with Gaussian line-shapes with a full-width at a half maximum of 0.3 eV. Gray: carbon, small white: hydrogen, red: oxygen, large white: titanium, and yellow: sulfur atom. Green and brown isosurfaces stand for signs opposite in amplitude.

visible region. Fig. 4(b) shows total and partial densities of states (DOS) together with the electronic distributions of the highest occupied molecular orbital (HOMO) and lowest unoccupied molecular orbital (LUMO) of the model complex. The energy of the LUMO was estimated to be -4.41 eV. This energy is very close to the energy of the bottom (-4.0 - -4.3 eV)[22] of the conduction band of anatase TiO_2. As shown by the partial DOS (blue dashed curve) of the titanium atoms, the unoccupied orbitals including the LUMO are distributed on the Ti atoms. As shown in Fig. 5, the LUMO and the second, third and forth lowest unoccupied orbitals (LUMO+1, LUMO+2 and LUMO+3, respectively) consist of the 3d orbitals of titanium atoms in the TiO_2 cluster. Thus, the unoccupied orbitals correspond to the conduction band of TiO_2. On the other hand, the HOMO is located at -6.29 eV much higher than the top (-7.2 – 7.5 eV) of the valence band of anatase TiO_2. As shown by the partial DOSs of the benzene ring (green dashed curve) and sulfur atoms (red dashed curve), the HOMO is the π orbital of BDT moiety weakly delocalized on the coordinated titanium atoms. As shown in Fig. 5, the second, third and forth lowest occupied orbitals (HOMO-1, HOMO-2 and HOMO-3, respectively) are also distributed on the BDT moiety delocalized on the TiO_2 cluster. As many of the calculated excitations in the visible region are attributed to electronic transitions between these occupied and unoccupied orbitals, the observed broad absorption band in Fig. 4(a) is attributed to interfacial charge-transfer transitions from the BDT to the

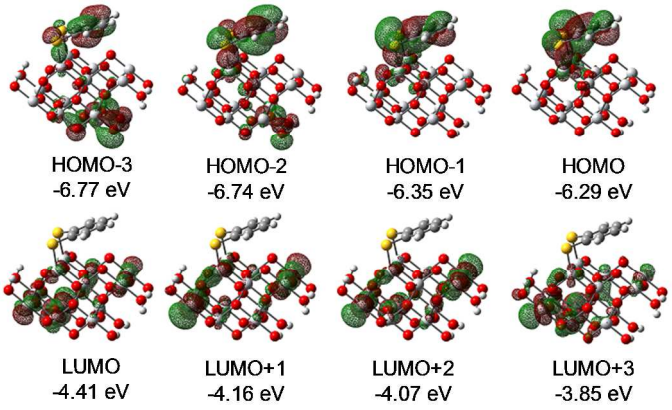

Fig. 5. Calculated electronic distributions (|isovalue| = 0.02) and energies of HOMO-3, HOMO-2, HOMO-1, HOMO, LUMO, LUMO+1, LUMO+2, and LUMO+3 of $[Ti_{12}O_{20}(OH)_6(\mu\text{-}S)_2$-benzene]. Green and brown isosurfaces stand for signs opposite in amplitude.

conduction band of TiO_2.

The contribution ratios of the benzene ring and sulfur and titanium atoms to the HOMO in the model complex were calculated to be 28, 57, and 11%, respectively, as shown in Fig. 4(b). This data indicates that the contribution of the 3p orbitals of the sulfur bridging atoms to the HOMO is much larger than that of the π orbital of the benzene moiety and the HOMO is delocalized on the titanium atoms via the sulfur atoms. For comparison, we carried out a similar DFT calculation of $[Ti_{12}O_{20}(OH)_6(\mu\text{-}O)_2$-benzene] with Ti-O-C linkages. The

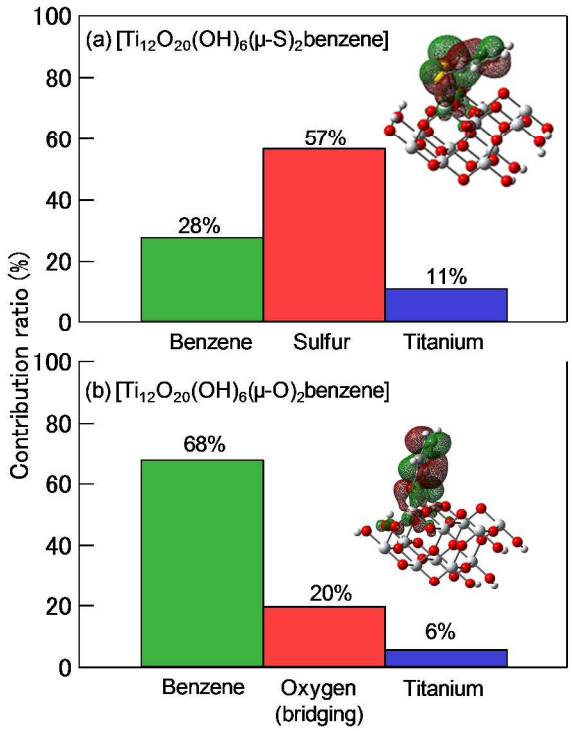

Fig. 6. Calculated contribution ratios of the benzene ring, bridging atoms and titanium atoms to HOMOs of (a) $[Ti_{12}O_{20}(OH)_6(\mu\text{-}S)_2\text{-benzene}]$ and (b) $[Ti_{12}O_{20}(OH)_6(\mu\text{-}O)_2\text{-benzene}]$ together with the electronic distributions (|isovalue| = 0.02).

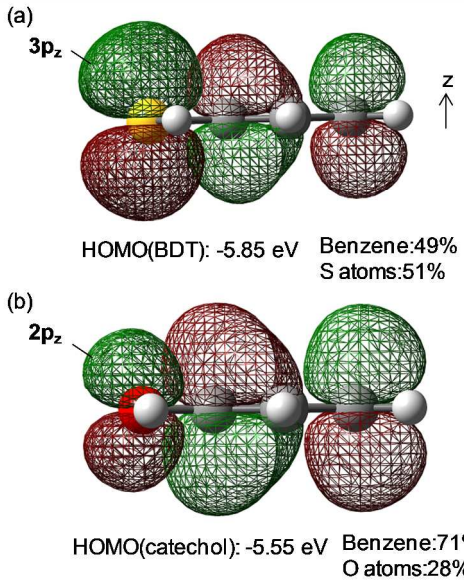

Fig. 7. Calculated electronic distributions (|isovalue| = 0.02) and energies of HOMOs of (a) BDT and (b) catechol together with the contribution ratios of the benzene ring and sulfur or oxygen atoms. Green and brown isosurfaces stand for signs opposite in amplitude.

optimized structure was calculated similarly with freezing the coordinates of all the titanium and oxygen atoms to those of anatase TiO_2. The contribution ratios of the benzene ring and bridging oxygen and titanium atoms to the HOMO were calculated to be 68, 20, and 6%, as shown in Fig. 6. The HOMO of $[Ti_{12}O_{20}(OH)_6(\mu\text{-}O)_2\text{-benzene}]$ is predominantly

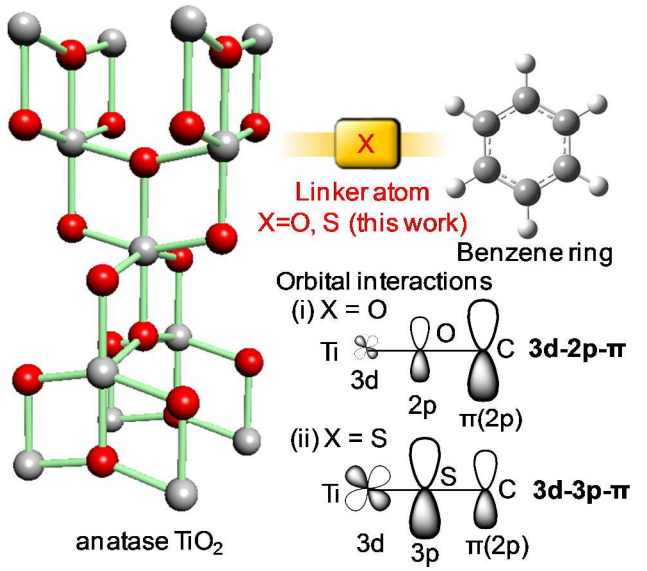

Fig. 8. Schematic picture of orbital interactions between TiO_2 and a benzene ring via oxygen or sulfur bridging atoms.

comprised of the π orbital of the benzene ring. Therefore, the wavefunction of HOMO is drastically changed by the sulfur bridging atoms. In addition, the ratio of the titanium atoms is considerably increased by the Ti-S-C bonds. This result indicates that the electronic hybridization is enhanced by the 3d-3p(S)-π interaction as compared to the 3d-2p(O)-π interaction. Fig. 7 shows the electronic distributions and energies of HOMOs of BDT and catechol. The HOMO of BDT is lower in energy than that of catechol. On the other hand, the contribution of the sulfur atoms in BDT is 51% that is much larger than that (28%) of the oxygen atoms. From these results, it can be seen that the enhanced electronic coupling between TiO_2 and a benzene ring is due to the $3p_z$ orbitals of the sulfur atoms with the larger spatial extent than the $2p_z$ orbitals of the oxygen atoms, as illustrated in Fig. 8.

Finally, we examined photovoltaic properties of the ICT transitions in the TiO_2-BDT complex. We fabricated electrochemical TiO_2-BDT based photovoltaic cells according to the method described in the Experimental section, as shown in Fig. 9(a). Fig. 9(b) shows an excitation spectrum of IPCE of the photovoltaic cell measured without any applied voltage. Photocurrent conversion due to the ICT transitions was observed in the visible region with an onset around 800 nm. This energy (1.55 eV) is very close to that (1.42 eV) of the calculated lowest electronic excitation in Fig. 4(a). The IPCE maximum value is about 25%. The diffuse reflectance spectrum in Fig. 2(b) indicates that about 60% of incident photons at 450 nm are not absorbed. The thickness (ca. 18 μm) of the TiO_2 photoanode is much lower than the sample (≳ ca. 1 mm) of the diffuse reflectance spectrum. For this reason, the lower IPCE values are considered to be due to the lower quantum efficiency of light absorption and the internal quantum efficiency is higher than 60%. This result indicates that injected electrons in TiO_2 due to the ICT transitions are effectively converted to current,

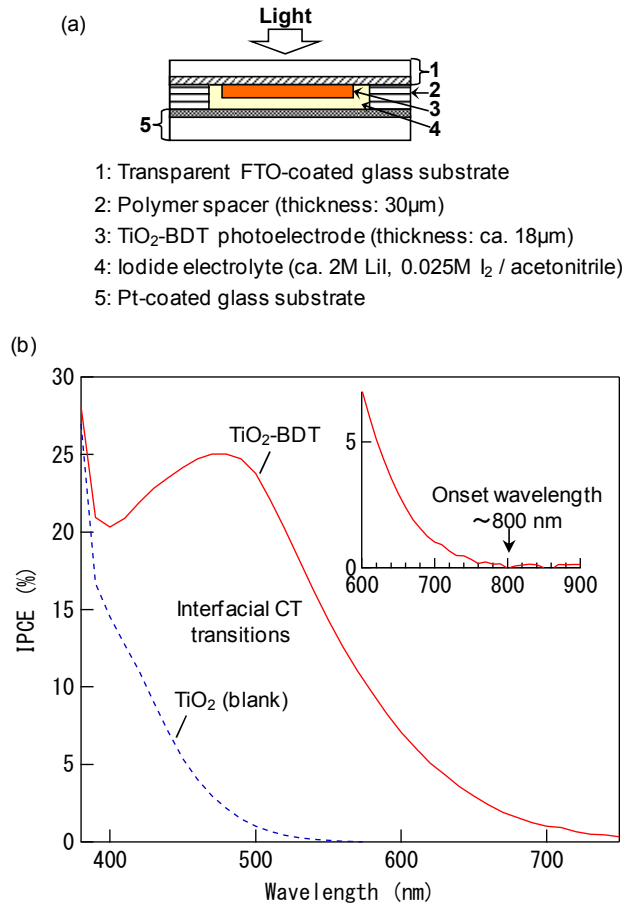

Fig. 9. (a) Structure of the electrochemical TiO_2-BDT photovoltaic cell and (b) IPCE excitation spectra of photovoltaic cells based on TiO_2-BDT (red solid curve) and TiO_2 (blank) (blue dashed curve) anodes with iodide electrolyte.

in contrast to the reported low internal quantum efficiency[4(e)] in the TiO_2-catechol complex. The enhancement in the internal quantum efficiency might be attributed to the suppression of carrier recombination[4(f)] from TiO_2 to the benzene moiety by the Ti-S-C linkage.

Conclusion

We reported ICT transitions in the TiO_2 and benzenedithiol complex with Ti-S-C linkages. The complex was formed by the bidentate Ti-S-C coordination and showed ICT transitions in the visible region. The ICT transitions induced the photovoltaic conversion showing relatively higher internal quantum efficiencies. In addition, our DFT analysis revealed that the electronic hybridization between TiO_2 and the benzene ring is enhanced by the 3d-3p-π interaction via the Ti-S-C linkage as compared to the 3d-2p-π interaction via the Ti-O-C linkage. This work demonstrated the important role of bridging atoms in organic-semiconductor electronic couplings and photovoltaic conversion due to ICT transitions.

Acknowledgements

This research was partially supported by the Precursory Research for Embryonic Science and Technology (PRESTO) program of the Japan Science and Technology Agency (JST) and Grant-in-Aid for Exploratory Research (Grant Number: 25620054) of Japan Society for the Promotion of Science (JSPS).

Notes and references

Graduate School of Science and Technology, Gunma University, 1-5-1 Tenjin-cho, Kiryu, Gunma, 376-8515, Japan. E-mail: jfujisawa@gunma-u.ac.jp

1 J. Fujisawa, M. Nagata and M. Hanaya, *Phys. Chem. Chem. Phys.*, in press, DOI: 10.1039/c5cp04456a.
2 J. Fujisawa and M. Nagata, *Chem. Phys. Lett.*, 2015, **619**, 180.
3 J. Fujisawa, *Phys. Chem. Chem. Phys.*, 2015, **17**, 12228.
4 (*a*) J. Moser, S. Punchihewa, P. P. Infelta and M. Grätzel, *Langmuir*, 1991, **7**, 3012; (*b*) R. Rodriguez, M. A. Blesa and A. E. Regazzoni, *J. Colloid Interf. Sci.*, 1996, **177**, 122; (*c*) P. Persson, R. Bergström and S. Lunell, *J. Phys. Chem. B*, 2000, **104**, 10348; (*d*) S. Ikeda, C. Abe, T. Torimoto, B. Ohtani, *J. Photoch. Photobio. A*, 2003, 61; (*e*) E. L. Tae, S. H. Lee, J. K. Lee, S. S. Yoo, E. J. Kang and K. B. Yoon, *J. Phys. Chem. B*, 2005, **109**, 22513; (*f*) Y. Wang, K. Hang, N. A. Anderson and T. Lian, *J. Phys. Chem. B*, 2003, **107**, 9434.
5 (*a*) Kubo, J. Fujisawa and H. Segawa, *Electrochemistry*, 2009, **77**, 977; (*b*) R. Jono, J. Fujisawa, H. Segawa and K. Yamashita, *J. Phys. Chem. Letters*, 2011, 2, 1167; (*c*) S. Manzhos, R. Jono, K. Yamashita, J. Fujisawa, M. Nagata and H. Segawa, *J. Phys. Chem. C*, 2011, **115**, 21487; (*d*) R. Jono, J. Fujisawa, H. Segawa and K. Yamashita, *Phys. Chem. Chem. Phys*. 2013, **15**, 18584. (*e*) J. Fujisawa and M. Hanaya, *Phys. Chem. Chem. Phys.*, 2015, **17**, 16285.
6 (*a*) M. Bledowski, L. Wang, A. Ramakrishnan, O. V. Khavryuchenko, V. D. Khavryuchenko, P. C. Ricci, J. Strunk, T. Cremer, C. Kolbeck and R. Beranek, *Phys. Chem. Chem. Phys*., 2011, **13**, 21511; (*b*) M. Bledowski, L. Wang, A. Ramakrishnan, A.lique Bétard, O. V. Khavryuchenko and R. Beranek, *ChemPhysChem*, 2012, **13**, 3018.
7 In our experiment, we examined the complex formation between TiO_2 and benzenethiol. We observed no coloration of TiO_2 nanoparticles by the addition of the solution of benzenedithiol. This result means that the adsorption of benzenedithiol onto TiO_2 via a Ti-S bond might be too weak and/or the probability of ICT transitions too low. Based on this result, we chose BDT with two thiol anchoring groups for stronger chemisorption to TiO_2 surfaces.
8 R. W. G. Wyckoff, *Crystal structures*, Vol. 1, John Wiely & sons, New York, London (1963).
9 H. Nakai, J. Heyd and G. E. Scuseria, *J. Comput. Chem. Jpn.*, 2006, **5**, 7.
10 W. Kohn and L. J. Sham, *Phys. Rev*., 1965, **140**, A1133.
11 (*a*) A.D. Becke, *J. Chem. Phys*., 1993, **98**, 5648; (*b*) C. Lee, W. Yang and R. G. Parr, *Phys. Rev. B*, 1988, **37**, 785.
12 (*a*) R. Ditchfield, W. Hehre and J. Pople, *J. Chem. Phys.*, 1971, **54**, 724; (*b*) W. Hehre, R. Ditchfield and J. Pople, *J. Chem. Phys.*, 1972, **56**, 2257.

13 M. A. L. Marques and E. K. U. Gross. *Annu. Rev. Phys. Chem.* 2004, **55**, 427.

14 M. J. Frisch *et al*. Gaussian 09, revision D.01; Gaussian, Inc.: Wallingford, CT, 2009.

15 N. M. O'boyle, A. L. Tenderholt and K. M. Langner, *J. Comput. Chem*., 2008, **29**, 839.

16 R. Beranek and H. Kisch, *Photochem. Photobiol. Sci*. 2008, **7**, 40.

17 In order to get an insight into the adsorption structure of BDT on TiO_2, the results reported for 1,2-benzenediol called catechol is helpful. It was reported that catechol chemisorbs on TiO_2 by the bridging bidentate Ti-O-C coordination via dehydration reactions between surface hydroxy groups on TiO_2 and two protons of the diol group and that the bidentate coordination is more stable than the monodentate coordination.[18,19] Giacomo *et al.* also reported that the Ti-O(H)-C coordination of the diol group with surface titanium atoms without dehydration reactions is also energetically favorable.[19] In addition, a chelating bidentate coordination of the diol group via dehydration reactions was suggested in the several papers.[4(a),4(b),4(e)] Accordingly, the adsorption structure of catechol has not yet been clarified completely. As described in Introduction, no coloration of TiO_2 nanoparticles was observed for benzenethiol. This result suggests that the coordination of only one thiol group does not induce the ICT transitions, indicating that the ICT transitions in the TiO_2-BDT complex are attributed to the bidentate coordination of BDT. In addition, generally, the proton dissociation constant of a thiol group is higher than that of a hydroxy group. From these facts, BDT is considered to adsorb on TiO_2 by bridging and chelating bidentate Ti-S-C coordinations with dehydration reactions between surface hydroxy groups on TiO_2 and two protons of the dithiol group for the ICT absorption. For this reason, in this work, we examined the bridging bidentate coordination as one of the possible adsorption structures of BDT.

18 L-M. Liu, S.-C. Li, H. Cheng, U. Diebold, and A. Selloni, *J. Am. Chem. Soc*., 2011, **133**, 7816.

19 G. Giorgi, J. Fujisawa, H. Segawa and K. Yamashita, *Phys. Chem. Chem. Phys.*, 2013,15, 9761.

20 (*a*) F. E. Hahn, T. Kreickmann and T. Pape, *Dalton Trans*., 2006, 769; (*b*) F. Hupka and F. E. Hahn, *Chem. Comm*., 2010, **46**, 3744.

21 M. W. Wong, *Chem. Phys. Lett.*, 1996, **256**, 391.

22 (*a*) I. Chung, B. Lee, J. He, R. P. H. Chang and M. G. Kanatzidis, *Nature*, 2012, **485**, 486; (*b*) H.-S. Kim, C.-R. Lee, J.-H. Im, K.-B. Lee, T. Moehl, A. Marchioro, S.-J. Moon, R. Humphry-Baker, J.-H. Yum, J. E. Moser, M. Grätzel and N.-G. Park, *Sci. Rep*., 2012, **2**, 591; (*c*) J. Zhang, C. Yu, L. Wang, Y. Li, Y. Ren and K. Shum, *Sci. Rep*., 2014, **4**, 6954; (*d*) J. T.-W. Wang, J. M. Ball, E. M. Barea, A. Abate, J. A. Alexander-Webber, J. Huang, M. Saliba, I. Mora-Sero, J. Bisquert, H. J. Snaith and R. J. Nicholas, *Nano Lett*., 2014, **14**, 724.